Ab initio pseudopotential studies of equilibrium lattice structures and phonon modes of bulk BC_3

Hong Sun
Department of Physics, Shanghai Jiao Tong University, Shanghai 200030, People's Republic of China

Filipe J. Ribeiro, Je-Luen Li, David Roundy, Marvin L. Cohen, and Steven G. Louie
Department of Physics, University of California at Berkeley, and Materials Sciences Division, Lawrence Berkeley National Laboratory, Berkeley, California 94720, USA

(Received 08 October 2002; revised manuscript received 29 September 2003; published 29 January 2004)

Different stacking arrangements of BC_3 layered crystals are studied with the use of the *ab initio* pseudopotential density-functional method. The total energies, lattice constants, electron energy band structures and density of states, as well as phonon frequencies are calculated for the possible bulk BC_3 structures obtained by full relaxations starting from different initial atomic configurations of *ABAB* (or *ABCABC*)$\cdots$ layer stacking. Two stable BC_3 structures, one semiconductor and the other metal, are obtained, which have lower total energies comparing with those of the structures proposed previously. Our calculations show that except for these two BC_3 structures, all the structures we studied, including the BC_3 structures proposed previously, have imaginary phonon frequencies corresponding to the relative, parallel motion of the adjacent BC_3 layers, indicating the instability of the layer stacking in these structures.

DOI: 10.1103/PhysRevB.69.024110 PACS number(s): 61.50.Ah, 71.20.−b, 71.15.Mb, 81.05.Zx

I. INTRODUCTION

Graphitelike, layered structure of bulk BC_3 was successfully synthesized more than 15 yr ago by the chemical reaction of benzene and boron trichloride at 800 °C.[1] Experiments[2] and *ab initio* calculations[3,4] suggested that the synthesized material consists of BC_3 layers with hexagonal symmetry [see the atomic arrangement of a single BC_3 layer in Fig. 1(a)]. However, how the BC_3 layers are stacked in the bulk material is still unclear. Previous *ab initio* local-density-approximation (LDA) calculations[3,4] predicted that bulk BC_3 is metallic due to the interaction between the adjacent BC_3 layers. It was also expected,[5,6] based on this prediction, that the multiple sheet, concentric BC_3 (n,n) nanotubes fabricated with the arc-discharge method are also metallic; however, the single-sheet BC_3 (n,n) nanotubes are semiconducting. These *ab initio* predictions[3,4] of the structural properties of BC_3 were based on a step-by-step structure relaxation procedure, where the structure of a single BC_3 layer was determined first; then the structure of bulk BC_3 was obtained by trying a few stacking configurations, with the interlayer distance $c/2$ determined by minimizing the total energy as a function of c. The relative displacement and structure of the layers were held fixed during the energy minimization procedure. These calculations did not explore all the possible low-energy structures of bulk BC_3.

In this paper, we report the results of *ab initio* LDA pseudopotential full relaxation studies of different layer stackings of bulk BC_3, to search for more stable structures of the material. The structures of BC_3 are determined by allowing all 16 atoms in the unit cell of the *ABAB*$\cdots$$BC_3$ layered structures to relax in all the directions simultaneously. As a comparison, two *ABCABC* $\cdots$$BC_3$ layered structures are also constructed and fully relaxed to their equilibrium structures. In addition to the total energies and density of states, phonon modes (at Γ) of each stationary structure obtained after the full relaxation are calculated to determine the stability of the obtained structures.

II. METHOD OF CALCULATION

The total energy of bulk BC_3 is computed using the LDA pseudopotential total-energy scheme with a plane-wave basis set.[7–9] The norm-conserving, Troullier-Martins pseudopotentials[10] are used with cutoff radii of 1.5 a.u. for all the atoms and orbitals. The electron wave functions are expanded in plane waves up to a cutoff energy of 80 Ry. The exchange-correlation functional used is that of Ceperley and Alder[11] as parametrized by Perdew and Zunger.[12] The energy

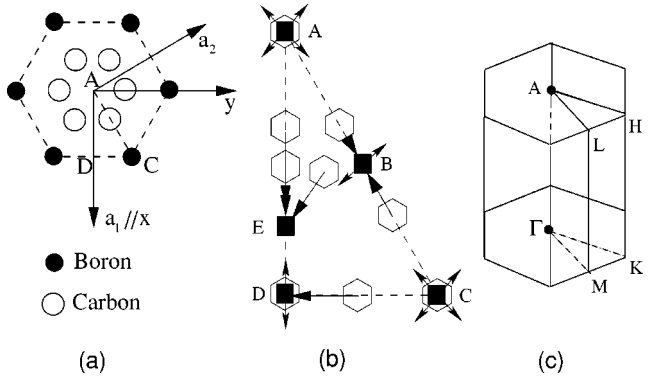

FIG. 1. (a) The unit cell on one BC_3 layer. (b) The hollow hexagons represent the initial center of the unit cell (CUC) of layer *B* relative to that of layer *A* before the structural relaxation, and the filled squares give the CUC of layer *B* of the stationary structure after the full relaxation for the *ABAB* . . . stacking structures. The one-arrow-end lines indicate the relaxation paths. The two-arrow-end lines give the polarization directions of the unstable phonon modes corresponding to the relative, parallel motion of the adjacent BC_3 layers. (c) The Brillouin zone and labeling of the reciprocal vector space of bulk BC_3.

TABLE I. Calculated structural parameters and phonon frequencies at Γ (in cm^{-1}) in graphite.

	a (Å)	$c/2$ (Å)	Ω_1	Ω_2	Ω_3	Ω_4	Ω_5
Our results	2.437	3.316	0	41*	110	900	1600
Other works	2.45 [a]	3.35 [a] (3.30 [b])					
Expt.	2.456[c]	3.337 [c]	0 [d]	45*,[d]	125 [d]	880 [e]	1600 [e]

[a]Reference 15.
[b]Reference 16.
[c]Reference 17.
[d]Reference 18.
[e]Reference 19.

of the structure is minimized by relaxing the structural parameters using a quasi-Newton method.[13] Phonon modes of the crystal structure are calculated with the linear response theory[14] using the ABINIT code for the equilibrium structures obtained after the structural relaxation. Test calculations for carbon in the graphite structure are carried out first. The results are given in Table I, in comparison with the previous *ab initio* calculations[15,16] and experiments.[17–19] The calculated LDA structural parameters and phonon frequencies (at Γ) agree very well with the measured values.[18,19] Although LDA cannot describe the van der Waals interactions between the layers, the accurate predictions on the interlayer distance $c/2$ and phonon frequency corresponding to the parallel relative motion of the layers (labeled with * in Table I) indicate that the short-ranged interlayer interactions in graphite are determined adequately by LDA,[15,16] which we believe is also true for BC_3 layered structures. The calculated (LDA) electron energy bands of graphite (not shown here) also agree well with those of previous calculations,[15] where the top of the occupied σ band lies 3.0 eV below the Fermi level.

III. RESULTS AND DISCUSSIONS

We first consider an $ABAB\ldots$ stacking of the BC_3 layered structure. The unit cell on one BC_3 layer (e.g., layer A) is chosen as that given in Fig. 1(a). Because of the hexagonal symmetry of the BC_3 layer, we can limit the center of the unit cell (CUC) on the adjacent layer (layer B) within the triangle ΔACD indicated in Fig. 1(a). Several initial CUC of layer B relative to that of layer A before the structural relaxation are given as the hollow hexagons in Fig. 1(b). The position at the corner A of ΔACD actually gives an $AAAA\ldots$ layered structure. The CUC of layer B of the stationary structure after the full relaxation are given as filled squares in Fig. 1(b). The one-arrow-end lines in Fig. 1(b) indicate the relaxation paths. We wish to point out that during the relaxation all the 16 atoms in the unit cell of bulk BC_3 are allowed to move freely, which is not the case in the step-by-step relaxations carried out in previous calculations[3,4] (see discussion below). The stationary structures obtained in Fig. 1(b) will be named hereinafter as BC_3-A, BC_3-B, $\ldots$, BC_3-E. The Brillouin zone (and labeling of the high-symmetry points) of bulk BC_3 is given in Fig. 1(c). From Fig. 1(b), it is seen that for BC_3-E, the displacement of layer B relative to layer A is about $\mathbf{a}_1/3$ in the $\overrightarrow{AD}$ direction. If we further shift the second-next BC_3 layer (layer C) relative to layer A by $2\mathbf{a}_1/3$ in the $\overrightarrow{AD}$ direction, we obtain an initial $ABCABC\cdots$ stacking BC_3 layered structure. This structure is named as BC_3-F. Similarly, another $ABCABC\ldots$ stacking BC_3 layered structure is obtained by shifting layer B and layer C relative to layer A by $(2\mathbf{a}_1+\mathbf{a}_2)/3$ and $2(2\mathbf{a}_1+\mathbf{a}_2)/3$ respectively in the $\overrightarrow{AC}$ direction. This structure is named as BC_3-G. The Brillouin zone of

TABLE II. Calculated total energies and structural parameters of BC_3.

	E (eV/atom)	$\mathbf{a}_1$ (Å)	$\mathbf{a}_1$ (Å)	$c/2$ (Å)	$\theta°$	$\bar{d}_{CC}$ (Å)	$\bar{d}_{BC}$ (Å)	x_0 (Å)	y_0 (Å)
A	−135.9074	5.110	5.110	3.674	120	1.403	1.547	0	0
B	−135.9183	5.114	5.114	3.177	120	1.404	1.549	1.279	0.737
C	−135.9086	5.111	5.111	3.421	120	1.404	1.547	2.555	1.475
D	−135.9203	5.123	5.113	3.168	120.1	1.406	1.547	2.561	0
E	−135.9294	5.123	5.116	3.105	120.1	1.405	1.550	1.780	0
F	−135.9280	5.120	5.110	3.154	120.1	1.406	1.551	1.781	0
G	−135.9122	5.110	5.110	3.430	120.0	1.404	1.545	2.553	1.473
A and C[a]		5.14	5.14	3.35	120	1.42	1.55		
B[b]		5.14	5.14	3.44	120	1.42	1.55		
Expt.				3.35[c]					

[a]Reference 3.
[b]Reference 4.
[c]Reference 1.

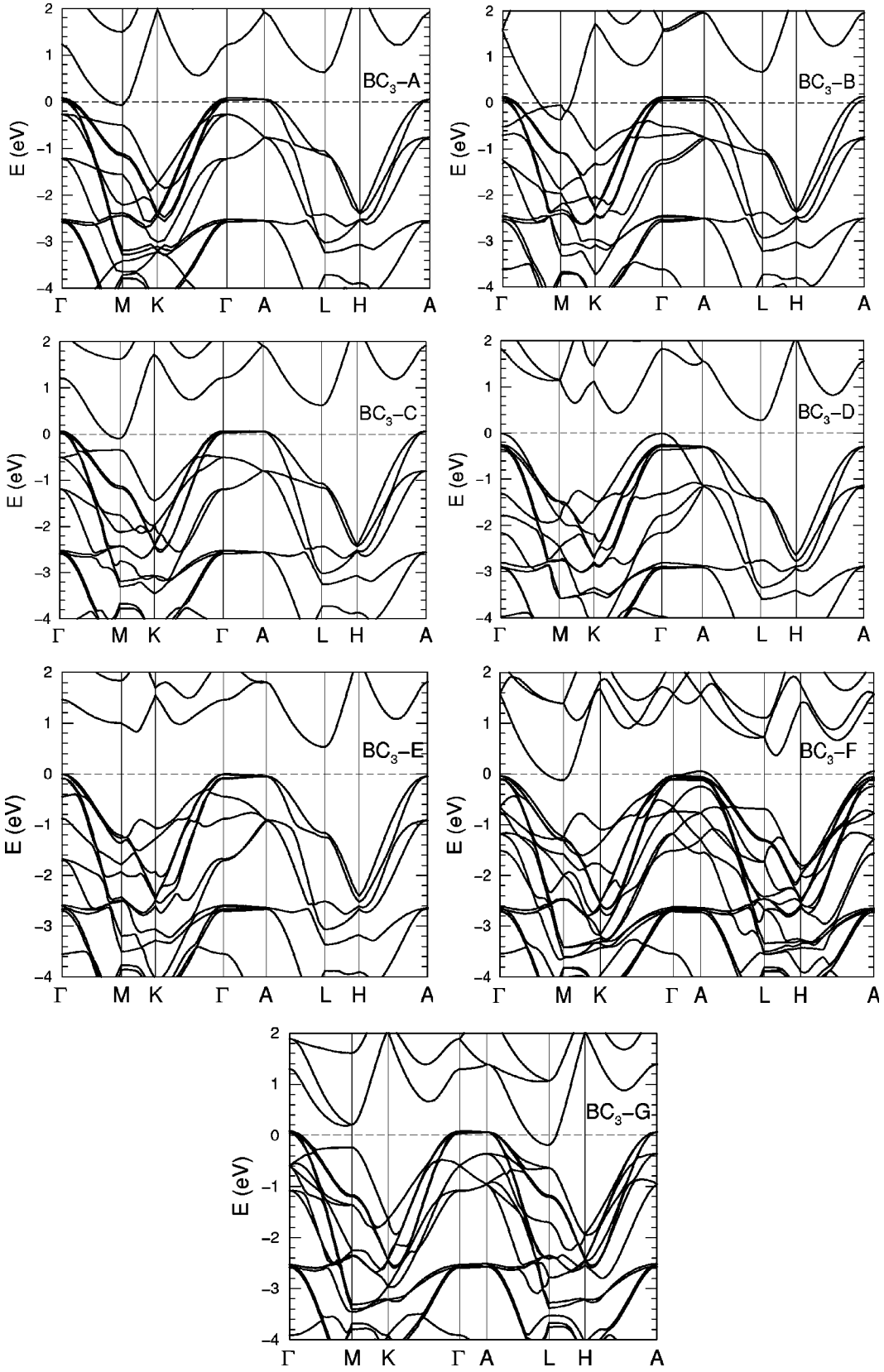

FIG. 2. The calculated electron energy bands of BC_3-*A*, . . . , BC_3-*G* described in Table II. The Fermi level is given by the dashed line at $E=0$.

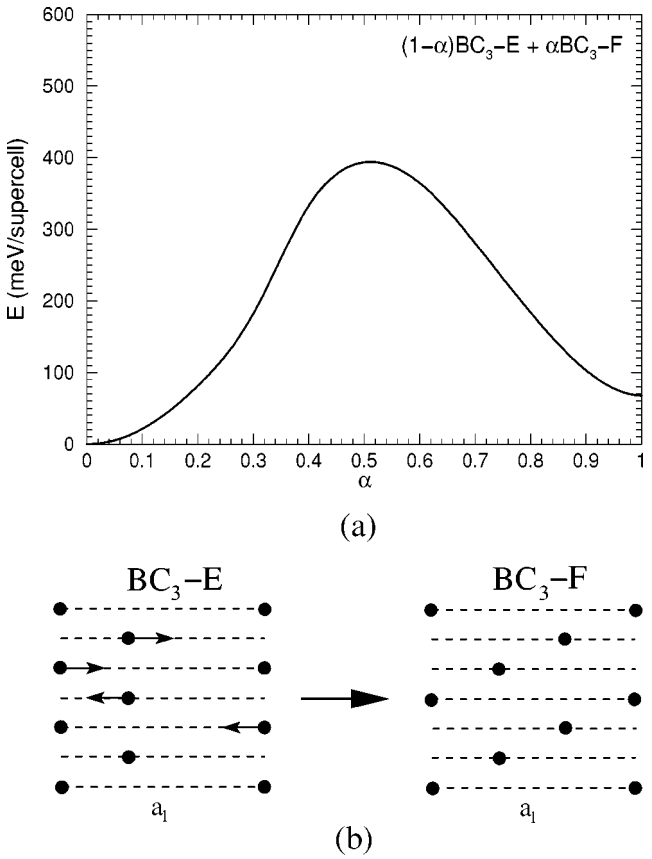

FIG. 3. (a) The total energy of a BC_3 six-layer supercell along one transition path from BC_3-*E* to BC_3-*F* described in Table II. (b) The six-layer supercell used to construct the transition path by a liner interpolation. The filled circles represent the center of the unit cell on each BC_3 layer along the $\mathbf{a}_1$ direction in Fig. 1(a). The movement of each layer is indicated in (b) by the small arrows on the filled circles in the structure of BC_3-*E*, which gives the shortest motion distance for each BC_3 layer to transform from BC_3-*E* to BC_3-*F*.

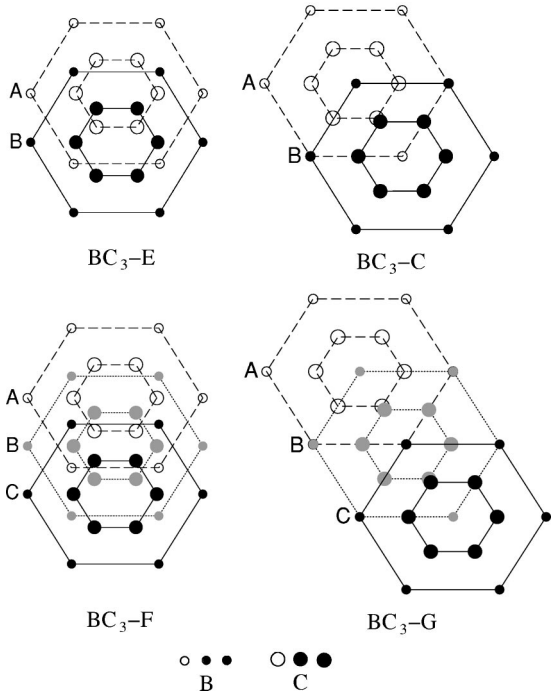

FIG. 4. The top view of the atomic positions of BC_3-*E*, BC_3-*F*, BC_3-*C*, and BC_3-*G*. The large (small) circles represent carbon (boron) atoms, and different darkness of the circles indicates different BC_3 layers.

BC_3-*F* and BC_3-*G* is similar to that shown in Fig. 1(c), except being shorter in the Γ-*A* direction.

The calculated results for the total energies *E*, the lattice vectors $\mathbf{a}_1$, $\mathbf{a}_2$, $\mathbf{c}$, and the angle θ between $\mathbf{a}_1$ and $\mathbf{a}_2$, the (average) in-plane C—C and C—B bond lengths $\bar{d}_{CC}$ and $\bar{d}_{CB}$, as well the CUC $(\mathbf{x}_0,\mathbf{y}_0)$ of layer *B* relative to layer *A* in the (x,y) plane are listed in Table II for all the stationary bulk BC_3 structures we obtained, together with the results of the previous calculations.[3,4] BC_3-*E* is expected to be the most stable structure, though the energy differences among the seven BC_3 structures are small, especially between BC_3-E and BC_3-*F*. The in-plane bond lengths we obtained are close to those of the previous *ab initio* calculations, which are nearly independent of how the BC_3 layers are stacked up. The interlayer distance $c/2$ (or $c/3$ for BC_3-*F* and BC_3-*G*) of bulk BC_3, however, depends strongly on the type of layer stacking. The interlayer distances we obtained for BC_3 are different from those of the previous calculations,[3,4] which may be due to the different relaxation procedures used in the calculations. In Ref. 3, the in-plane bond lengths were obtained by relaxing a single BC_3 layer. Then bulk BC_3-*A* and BC_3-*C* structures were constructed by fixing the interlayer distance at the experimental value $c/2=3.35$ Å.[1] In Ref. 4, the in-plane bond lengths were obtained first with the interlayer distance fixed at $c/2=3.35$ Å. Then the interlayer distance was obtained by minimizing the total energy with respect to c for BC_3-*B* and BC_3-*C* with the in-plane bond lengths held fixed. An interlayer distance $c/2=3.44$ Å was obtained for BC_3-*B*. While for BC_3-*C*, it was found in Ref. 4 that the total energy decreases monotonically as *c* increases, hence no stable structure was found. One should note that the BC_3-*B* structure studied in Ref. 4 was constructed by arbitrary movement of the BC_3 interlayers, while that we studied was obtained by structural relaxations. To our knowledge, the BC_3-*D* to BC_3-*G* structures have not been studied previously. The difference in the calculated interlayer distances between our results and those of previous calculations probably arises from the fact that in our calculation more plane waves (or higher cutoff energies) are used and we allow the atoms, especially the relative displacement of the BC_3 layers, to relax freely from the initial configurations with lower symmetries, such as BC_3-*E* and BC_3-*F*, etc. The interlayer distances of bulk BC_3 structures we obtained are all different from that reported in the experiment.[1] The explanation may be that as all the BC_3 structures have very close total energies, defects or impurities in the sample can make any of the structures become metastable. The experimental result may be that of a mixed structure.

In Fig. 2, the calculated electron energy bands of the seven BC_3 structures in Table II are shown. In order to make comparisons between the structures, the Brillouin zone of

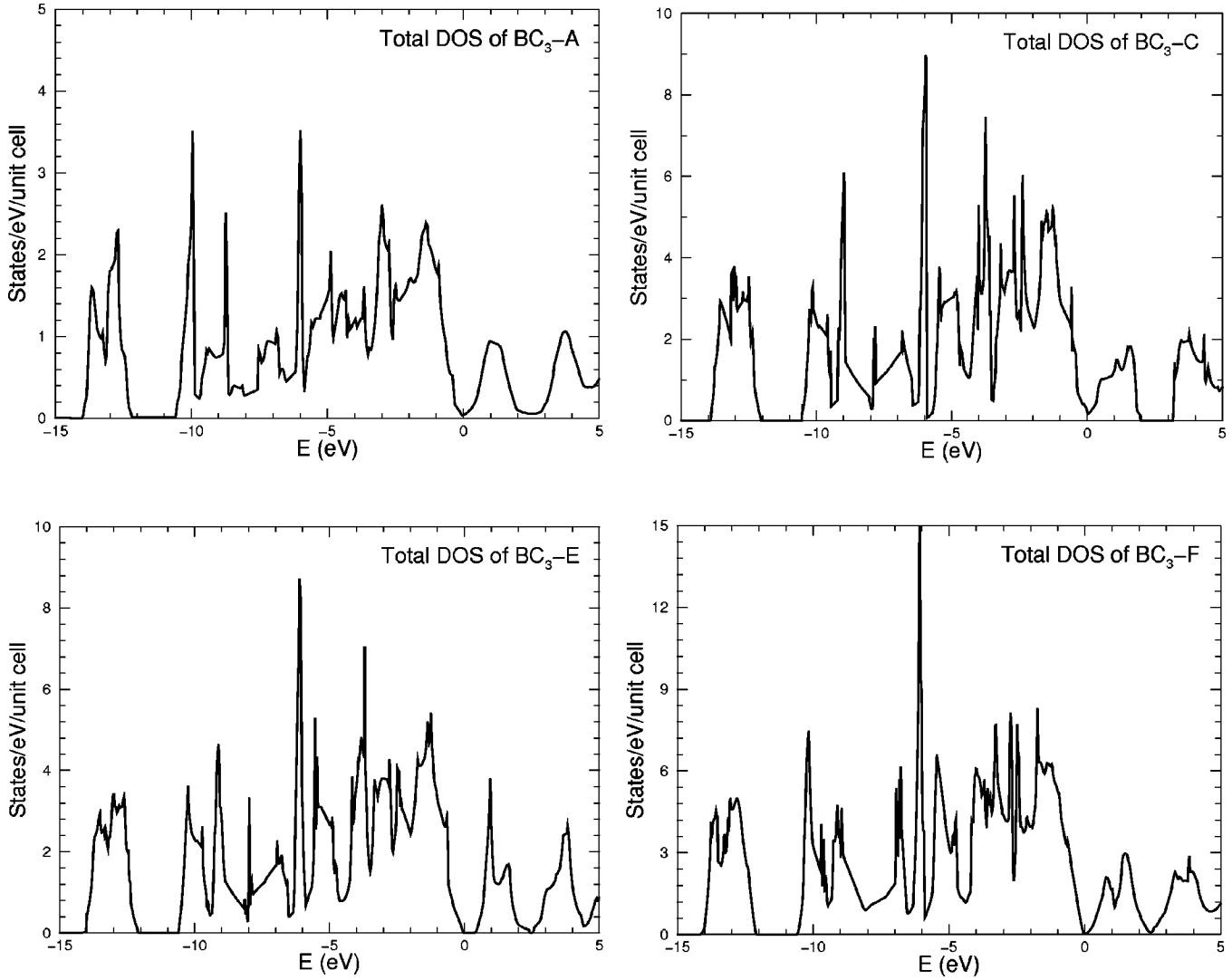

FIG. 5. The calculated total electron density of states as a function of energy for BC_3-*A*, BC_3-*C*, BC_3-*E*, and BC_3-*F*. The Fermi level is set at $E=0$.

BC_3-*A* was folded in half in the $\mathbf{b}_3$ direction. The results clearly show that BC_3 changes from a metal (for BC_3-*A*, . . . , BC_3-*C*) to a semiconductor (for BC_3-*D* and BC_3-*E*) and to a metal again (for BC_3-*F* and BC_3-*G*). An indirect LDA band gap $E_g \approx 0.5$ eV is estimated for BC_3-*E*, which is expected to be less than that of the real material since LDA tends to underestimate the energy gap. The metallic behavior of the BC_3 sample observed in the experiment[1] is again attributed to the suggestion that the sample measured has a mixed structure, especially the mixture of the semiconductor structure BC_3-*E* and the metallic structure BC_3-*F* due to the small energy difference between these two structures. Similar mixed *ABAB* . . . and *ABCABC* . . . stacking layered structures were also found in natural graphite.

In Fig. 3(a), we plot the total energy of a BC_3 6-layer supercell along one transition path from BC_3-*E* to BC_3-*F*. The transition path is constructed by a linear interpolation $BC_3 = (1-\alpha)BC_3$-$E + \alpha BC_3$-*F*, using a six-layer supercell as shown in Fig. 3(b), where the filled circles represent the center of the unit cell on each BC_3 layer along the $\mathbf{a}_1$ direction sketched in Fig. 1(a). The movement of each layer is indicated in Fig. 3(b) by the small arrows on the filled circles in the structure of BC_3-*E*, which gives the shortest motion distance for each BC_3 layer to transform from BC_3-*E* to BC_3-*F*. The low energy barrier ($\sim$10 meV/atom) shows the easiness for BC3 structure to shift between BC_3-*E* and BC_3-*F*.

The layer stacking of the preferred structures of BC_3-*E* and BC_3-*F* we obtained are very different from that of the possible stable structures of graphite, where structures similar to BC_3-*C* and BC_3-*G* are found in the natural graphite. In Fig. 4, we give the top view of the atomic positions of BC_3-*E*, BC_3-*F*, BC_3-*C* and BC_3-*G*, where the large (small) circles represent carbon (boron) atoms, and different darkness of the circles indicates different BC_3 layers. Obviously, atoms of different BC_3 layers in the stable structures (BC_3-*E* and BC_3-*F*) avoid stacking on top of each other. This can be explained as follows: The boron atoms in a single BC_3 layer weaken the interactions of p_z states (z parallel to the c axis) of neighboring carbon rings, and reduce the dispersion of the

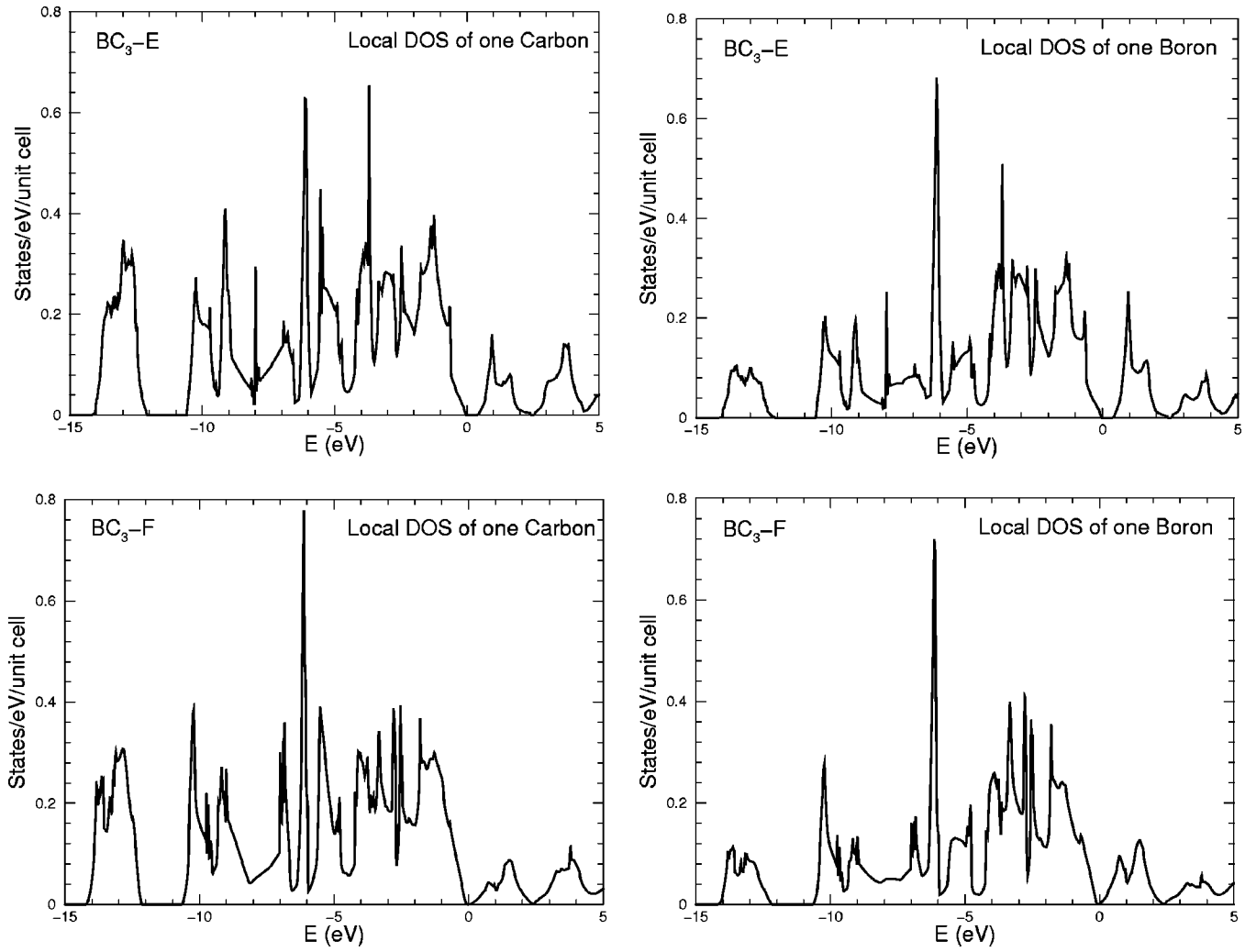

FIG. 6. The calculated local electron density of states as a function of energy for the carbon and boron atoms in BC_3-*E* and BC_3-*F*. The Fermi level is set at $E=0$.

π bands so that the Fermi level of a single BC_3 layer lies below the π bands.[3] The interlayer interaction will increase the dispersion of the π bands. For BC_3 structures where atoms (or part of atoms) in each layer stack on top of each other, such as BC_3-*A* or BC_3-*C*, the layer interaction is strong enough to move the dispersion of one of the π bands below the Fermi level from above. The structures become metallic (see Fig. 2, BC_3-*A* or BC_3-*C*), and have higher total energies as more electrons occupy states near the Fermi level. While for BC_3-*E*, where atoms of different layers avoid stacking on top of each other, the layer interaction is weaker and the π bands remain above the Fermi level. The structure is a semiconductor with lower total energy since fewer electrons occupy states near the Fermi level. The increase of the total energy of bulk BC_3 when part of the atoms of the adjacent layers stack on top of each other is also clearly illustrated in Fig. 3, where the total energy of the supercell reaches its maximum when the BC_3 layers move half way ($\alpha=0.5$) from BC_3-*E* to BC_3-*F* with atoms of most of the adjacent layers lying on top of each other. Different layer stacking also changes the electron band structures of bulk BC_3 by the effect of the Brillouin-zone folding. Comparing the electron band structures of BC_3-*C* (*ABAB* . . . stacking) and BC_3-*G* (*ABCABC* . . . stacking) in Fig. 2, the folding of the Brillouin zone exchanges the characters of the π bands at *M* and *L* points between BC_3-*C* and BC_3-*G*, and lower the bottoms of these bands. The same effect happens between BC_3-*E* (*ABAB* . . . stacking) and BC_3-*F* (*ABCABC* . . . stacking), with a sufficient lowering of the π bands to make BC_3-*F* become a (LDA) metal.

In Fig. 5, we plot the calculated total electron density of states (DOS) for BC_3-*A*, BC_3-*C*, BC_3-*E*, and BC_3-*F*. Two peaks of the π bands separated by about 3 eV are found above the Fermi level for all the bulk BC_3 structures we studied. The noticeable difference is that these peaks are sharper and stronger in BC_3-*E*. Experimentally, electron transitions from 1*s* states to the π bands are observed in the electron energy-loss spectrum (EELS) of bulk BC_3 at sub-eV resolution.[2] The fine structure of the *boron K*-edge spectra of the EELS shows two sharp peaks separated by 2.6 eV, which are assigned to the excitation of electrons from the 1*s* states to the unoccupied levels in the conduction bands, and agrees

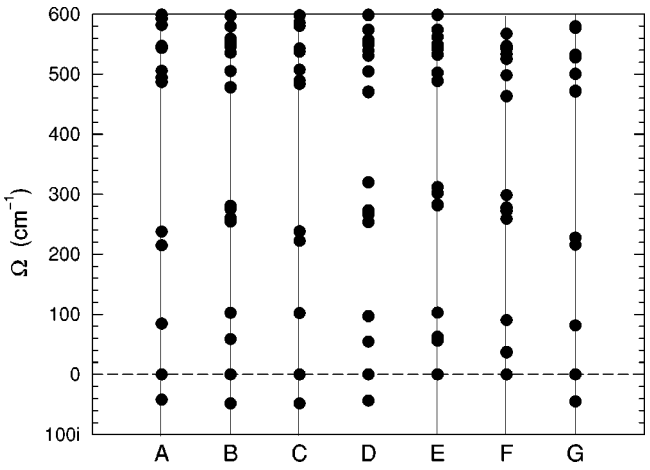

FIG. 7. The calculated phonon frequencies (at Γ) of BC_3-*A*, . . . , BC_3-*G* described in Table II are given along the straight lines *A*, . . . ,*G*, respectively. The Brillouin zone of BC_3-*A* is folded in half in the $\mathbf{b}_3$ direction, where the phonon frequencies include both Γ and *A* phonons of the original Brillouin zone of BC_3-*A*. The obtained values of the phonon frequencies are indicated by the filled circles. The imaginary frequencies are displayed below $\Omega = 0$.

well with the splitting of the π bands above the Fermi level in the calculated total DOS of bulk BC_3. However, only *one* peak is observed experimentally in the carbon *K*-edge spectra. In Fig. 6, we plot the calculated local DOS of the carbon and boron atoms for BC_3-*E* and BC_3-*F*. The local DOSs of the other BC_3 structures we studied are similar as can be seen from their total DOS's in Fig. 5. The results show that double π band peaks are expected for both carbon and boron local DOS's; only the double π peaks are much pronounced for the boron local DOS in BC_3-*E*. Theoretical calculations of the EELS for the BC_3-*C* structure were reported based on the multiple scattering approach,[20] which also predicted a double π peak for the boron *K*-edge spectra separated by 3.5 eV and a single π peak for the carbon *K*-edge spectra. This seems to indicate that the excitation of 1*s* electrons in carbon to one of the two π bands in the conduction bands is somehow ''forbidden.''

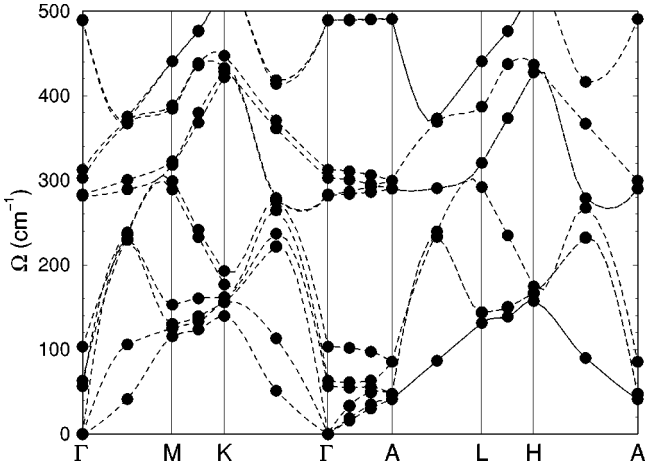

FIG. 8. The calculated phonon bands of BC_3-*E*. The obtained values of the phonon frequencies are indicated by the filled circles. The dashed lines are the smooth fitting curves of the calculated phonon bands.

To clarify how to classify the stationary structures (local minimum, maximum, or saddle point), we calculated the phonon modes (at Γ) for each of the seven BC_3 structures in Table II. The results are given in Fig. 7. Again the Brillouin zone of BC_3-*A* was folded in half in the $\mathbf{b}_3$ direction, where the phonon frequencies include both Γ and A phonons of the original Brillouin zone of BC_3-*A*. The calculated values of the phonon frequencies are indicated by filled circles. Imaginary phonon frequencies are found for all the BC_3 structures, except for BC_3-*E* and BC_3-*F*. The polarizations of these unstable phonon modes correspond to the parallel ''vibrations'' of the adjacent BC_3 layers, as indicated by the two-arrow-end lines in Fig. 1(b) for the *ABAB* . . . stacking structures. It is clear from Fig. 1(b) that BC_3-*A* and BC_3-*C* are at a local maximum, BC_3-*B* and BC_3-*D* are at a saddle point, and BC_3-*E* is the only stable structure that we find for the *ABAB* . . . BC_3 layered structure. For the *ABCABC* . . . stacking structures we studied, BC_3-*F* is stable, while BC_3-*G* is at a local maximum. The full phonon bands for BC_3-*E* are given in Fig. 8 which shows that all the phonon frequencies are real.

IV. CONCLUSIONS

Different stacking arrangements of BC_3 layered crystals are studied with the use of the *ab initio* LDA pseudopotential density-functional method. The total energy, lattice constants, electron energy band structures, and density of states, as well as phonon frequencies are calculated for all the possible bulk BC_3 structures obtained after full relaxations starting from different initial atomic configurations of *ABAB* . . . and *ABCABC* . . . stacking. The metallic structural forms BC_3-*A*, BC_3-*B*, and BC_3-*C* proposed for bulk BC_3 in the previous *ab initio* calculations[3,4] are found to be unstable with their phonon frequencies corresponding to the relative, parallel motion of the adjacent BC_3 layers being imaginary. Two stable structures are obtained for the *ABAB* . . . and *ABCABC* . . . BC_3 layered structures, which have real frequencies for all phonon modes and lower total energies among all the structures we studied, even though the energy differences are small. One of the stable structures (BC_3-*E*) is expected to be a semiconductor with an indirect (LDA) band gap of about 0.5 eV, and the other (BC_3-*F*) is a (LDA) metal. The interlayer distance of the stable bulk BC_3 structures we obtained is about 7% smaller than that reported in the experiment.[1] This discrepancy may indicate that the measured sample is a mixed structure caused by defects and impurities. The same speculation of a mixed structure may be used to explain the experimentally observed metallic behavior of the sample and our predicted semiconducting band structure for one of the stable bulk BC_3 structures.

ACKNOWLEDGMENTS

This work was supported by National Science Foundation Grant No. DMR-0087088, by the Director, Office of Energy Research, Office of Basic Energy Sciences, Materials Sci-

ences Division of the U. S. Department of Energy, and the Laboratory Directed Research and Development Program of Lawrence Berkeley National Laboratory under the U.S. Department of Energy. Computational resources were provided by the National Science Foundation at the National Center for Supercomputing Applications and by the National Energy Research Scientific Computing Center. All Department of Energy support was under Contract No. DE-AC03-76SF00098. H. S. acknowledges the financial support from the National Natural Science Foundation of China Grant No. 10274050, the Tang Family Foundation, and the support of computational resources from the High Performance Computing Center at Shanghai Jiao Tong University.

[1] J. Kouvetakis, R.B. Kaner, M.L. Sattler, and N. Bartlett, J. Chem. Soc., Chem. Commun. **1986**, 1758 (1986).
[2] K.M. Krishnan, Appl. Phys. Lett. **58**, 1857 (1991).
[3] D. Tomanek, R.M. Wentzcovitch, S.G. Louie, and M.L. Cohen, Phys. Rev. B **37**, 3134 (1988).
[4] Q. Wang, L.Q. Chen, and J.F. Annett, Phys. Rev. B **54**, R2271 (1996); **55**, 8 (1997).
[5] Y. Miyamoto, A. Rubio, S.G. Louie, and M.L. Cohen, Phys. Rev. B **50**, 18 360 (1994).
[6] Z. Weng-Sieh, K. Cherrey, N.G. Chopra, X. Blase, Y. Miyamoto, A. Rubio, M.L. Cohen, S.G. Louie, A. Zettl, and R. Gronsky, Phys. Rev. B **51**, 11 229 (1995).
[7] J. Ihm, A. Zunger, and M.L. Cohen, J. Phys. C **12**, 4409 (1979).
[8] D.M. Ceperley and B.J. Alder, Phys. Rev. Lett. **45**, 566 (1980).
[9] M.L. Cohen, Phys. Scr., T **1**, 5 (1982).
[10] N. Troullier and J.L. Martins, Phys. Rev. B **43**, 1993 (1991).
[11] D.M. Ceperley and B.J. Alder, Phys. Rev. Lett. **45**, 566 (1980).
[12] J.P. Perdew and A. Zunger, Phys. Rev. B **23**, 5048 (1981).
[13] B.G. Pfrommer, M. Côté, S.G. Louie, and M.L. Cohen, J. Comput. Phys. **131**, 233 (1997).
[14] X. Gonze, Phys. Rev. B **55**, 10 337 (1997); X. Gonze and C. Lee, *ibid.* **55**, 10 355 (1997).
[15] M.C. Schabel and J.L. Martins, Phys. Rev. B **46**, 7185 (1992).
[16] J.C. Charlier, X. Gonze, and J.P. Michenaud, Europhys. Lett. **28**, 403 (1994).
[17] Y. Baskin and L. Mayer, Phys. Rev. **100**, 544 (1955).
[18] R. Nicklow, N. Wakabayashi, and H.G. Smith, Phys. Rev. B **5**, 4951 (1972).
[19] G. Benedek, F. Hofman, P. Ruggerone, G. Onida, and L. Miglio, Surf. Sci. Rep. **20**, 1 (1994).
[20] M. Wibbelt, H. Kohl, and P.K. Redlich, Phys. Rev. B **59**, 11 739 (1999).